PARAMETRIC ANALYSIS OF ABRASIVE WATER JET MACHINING

Shrirang chandrakant kanade, J.B.Shaikh

Dr. Babasaheb Ambedkar Technological University Lonere, Dist.- Raigad, Maharashtra, India

Department of Mechanical Engineering, Deogiri Institute of Engineering and Management Studies, Aurangabad

ABSTRACT

The present research work highlights the simulation study of AWJM process parameters, i.e. velocity of jet, Jet impingement angle, grain size and stand-off-distance on pressure, stress and Deformation generated at the jet impact surface, erosion rate during the fabrication of micro holes generation. K-60 Ceramic is widely accepted in the non-conventional machining process and associated industries with the years of track on record of proven performance in a vast number of brittle materials. The intense hardness and high strength of sintered ceramics creates it tough to machine them economically. The present surface development models are established for air abrasive driven erosion progressions which cannot account for the result of heated abrasive movement on the target channel sidewall erosion that indicates to the advanced channel broadening detected in the AWJM of brittle materials. This paper focused on ideal numerical model to predict the surface contours of micro-holes in brittle material as name K-60 ceramic using AWJM. Most perceptible act in this research is to the selection of abrasive particle that for to achieve the appropriate intricate shaped holes upon K-60 ceramic with silicon carbide abrasives. The exact erosion rates of this material, pressure, stress generation and deformation due to stresses are measured.

Keywords, *K-60 ceramic, 3-D CFD model, SiC abrasive, AWJM, ANSYS 18.1 CFX.*

1. INTRODUCTION

ABRASIVE WATER JET MACHINING PROCESS

In our current research work we are focusing on Mechanical based Non-Traditional Manufacturing process, i.e. Abrasive water jet manufacturing process. . In these processes higher kinetic energy of abrasive particles jet and water jet is employed for removing materials from the work piece. In abrasive water jet machining process material removal takes from the surface of work material because of the impact of high velocity and pressure of water/abrasive jet on it and the energized particles generates stresses on it and due to stresses brittle fracture forms at that surface and due to the subsequent impact of abrasive particles material removal occurs. The schematic diagram of abrasive water jet machining is displayed below.

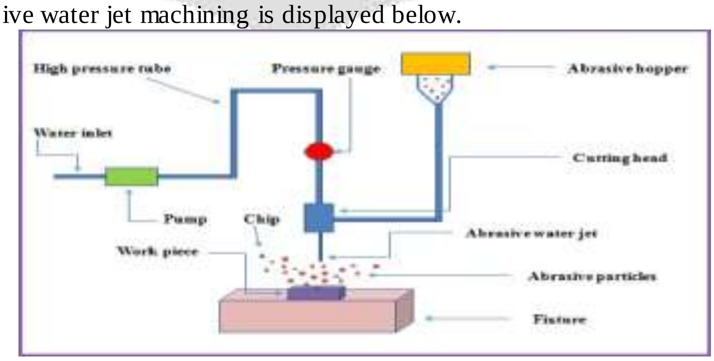

Fig.1. Schematic Diagram of AWJM machining process

2. BOUNDARY CONDITIONS USED FOR SIMULATION:

pressure based system, steady state and incompressible flow condition with energy method, k-epsilon turbulence model ,Discrete phase model (DPM) and PISO scheme is used in ANSYS FLUENT 18.1 CFD tool for injecting the hot abrasive jet on to the work piece as per the design in Design modeler. Before initialization of flow and calculating the result in the solver unit the input flow parameter for the jet and the properties of work piece material and abrasive particles has been assigned at the cell zone condition as well as in boundary condition which is shown in Table 6 for getting the simulation output responses.

Table 1: Flow, solver setting and model parameter

Flow and model parameter	**Value**
Mass flow rate	0.01 kg/sec
Inlet velocity of jet	250 m/s, 280 m/s, 310 m/s, 340 m/s
Jet Impact Angle	65^oC , 75^oC, 90^oC, 105^oC
Abrasive particle diameter	245 µm , 445 µm, 645 µm, 845 µm
Stand-off distance	4 mm , 6 mm, 8 mm, 10 mm
Pressure velocity coupling	PISO
Momentum	2^{nd} Order
Turbulent kinetic energy	2^{nd} Order
Turbulence dissipation rate	2^{nd} Order
Skewness correction	0
Neighbor correction	3
Model	Energy and DPM model
Turbulence model	K –epsilon turbulence model

3. CFD MODELLING

Geometric modeling

Geometric modeling is the introductory phase in CFD simulation which develops the simulation flow field. Often making the geometry a simpler one, trying to restrict the geometry to the field that includes fluid flow, and avoiding the finer details in the layout. Intricate specifics make grid generation and simulation difficult. Novel design of Tungsten carbide (WC) nozzle with dimension and figure shown in Table 2.

Table 2: Geometric parameter of nozzle

Geometric parameter	**Dimension**
Inlet diameter	10 mm
Outlet diameter	4 mm
Focus tube length	21 mm
Convergent angle	2090
Converging length	7.0 mm
Body length	20 mm
Total Nozzle Length	48 mm

K-60 Alumina ceramic work piece of size 40×40×2 is designed at a certain distance stand-off distance (from the exit surface of nozzle) along with frozen operation for maintaining the gap between nozzle exit and work piece for making the nozzle and frozen body in to a single body at desired plane using the suitable coordinate system in design modeler

Discretization and Grid Generation

The methods to Discretization/meshing are used to transform a mathematical model into a discrete, algebraic equation system. There are typically three types of methods that are used to discrete. Finite element method (FEM) is used for stress analysis, but fluid flows use finite difference method (FDM) and finite volume method (FVM) is used for industrial CFD codes
Here the equation of motion of AWJM is solved by CFD tool ANSYS Fluent. The assembly of nozzle body and the work piece is discretized in to 1 mm element size along with 87655 no of element of tetrahedral mesh after the Boolean operation in Design modeler shown in Figure 02.

Fig.2: Discretization at different Impact angle

4. RESULT AND DISCUSSION

4.1 Effect of Velocity of Jet, Grain Size of Abrasive, Stand-Off-Distance, and Impact angle of Abrasive jet on Pressure on the Impact Surface of Jet on the Work Piece:

Taguchi is a strategy for defining and developing knowledge scientifically, so that it can be used in a well structured manner to improve the machining process. According to the definition, DOE can be applied to the regions where it is necessary to acquire and apply the information efficiently and quickly in any field of requirements. Here, Table 3 represents the Taguchi design matrix for simulation. According to this the simulation result of pressure profile at the impact surface of work piece has been displayed below in Figure 3-4.

Table 3: Taguchi simulation matrix for simulated pressure value at target zone.

Run No	Angle	Velocity	SOD	Grain Size	Pressure (In Mpa)
1	65	250	4	245	0.9321
2	65	280	6	445	0.9856
3	65	310	8	645	1.1065
4	65	340	10	845	1.3124
5	75	250	6	645	1.6321
6	75	280	4	845	1.5672
7	75	310	10	245	1.2654
8	75	340	8	445	1.789
9	90	250	8	845	1.923
10	90	280	10	645	1.2123
11	90	310	4	445	2.1126
12	90	340	6	245	2.0234
13	105	250	10	445	1.8753
14	105	280	8	245	1.7765
15	105	310	6	845	1.8623
16	105	340	4	645	2.0211

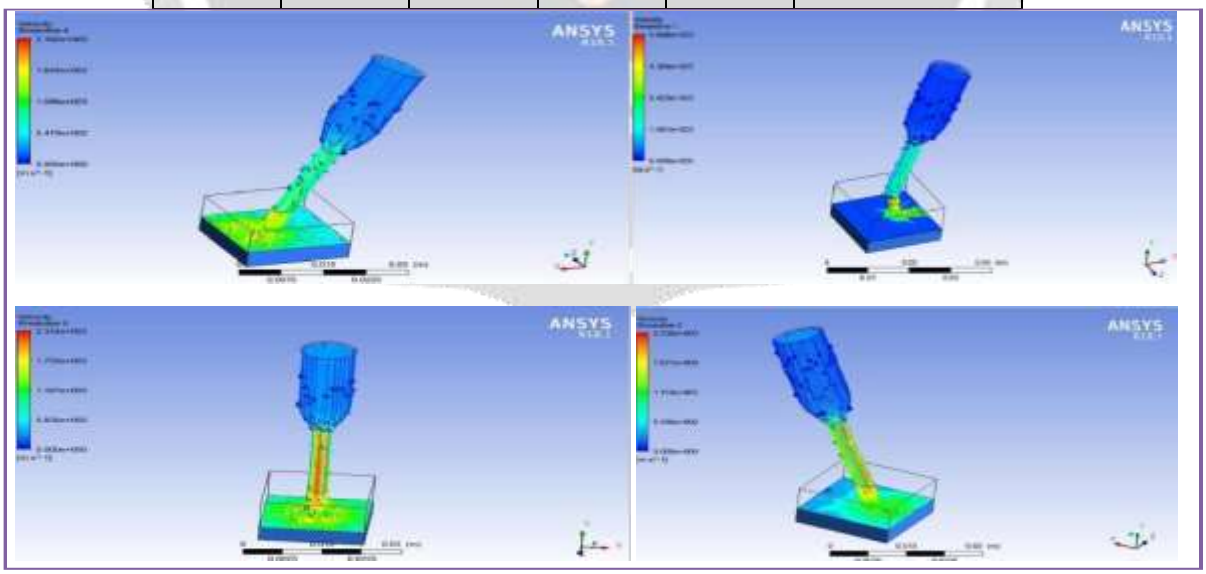

Fig.3 Velocity Profile and Contour at different Parameter

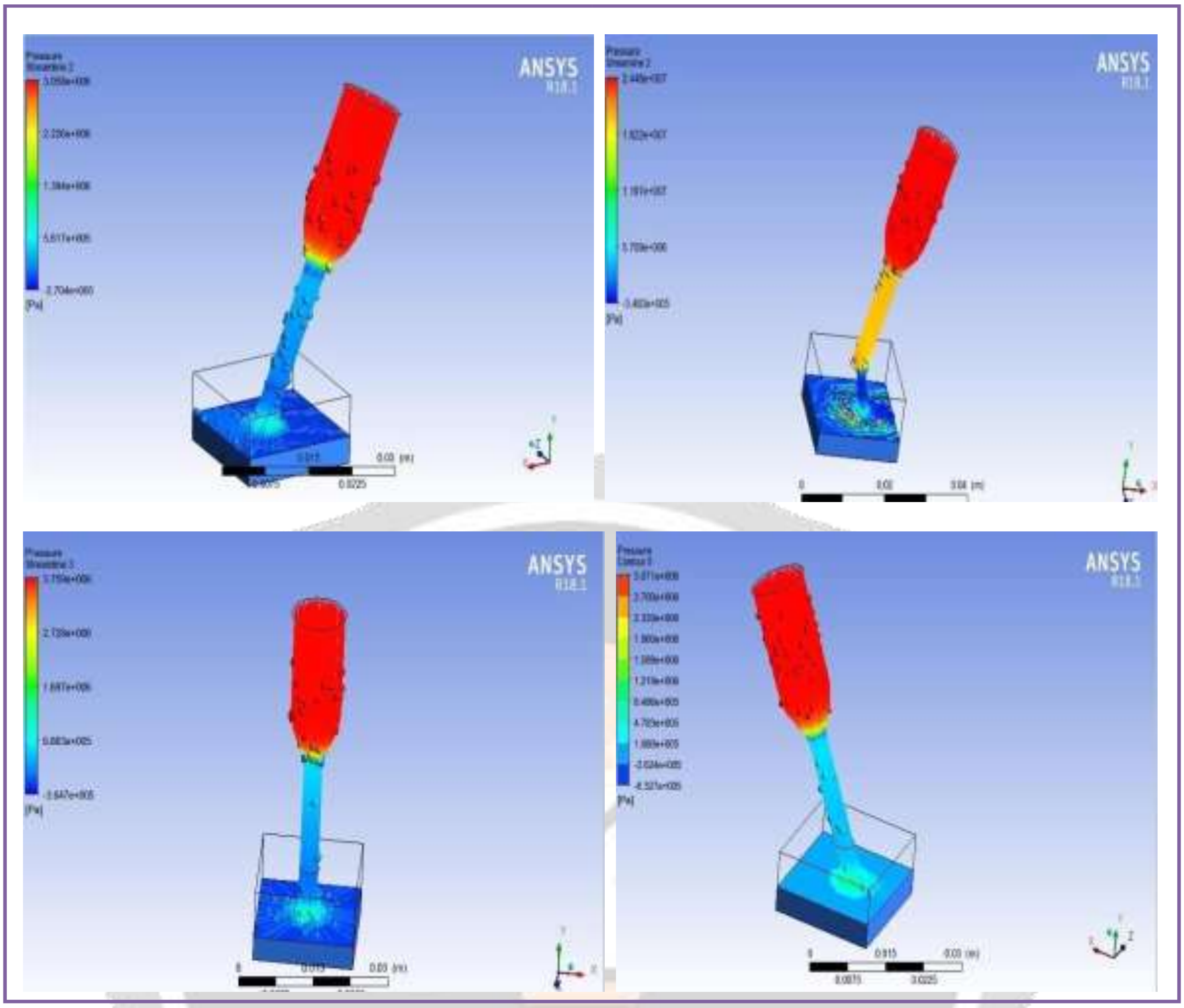

Fig.4 Pressure Profile and Contour at different Parameter

4.2 Effect of Velocity of Jet, Grain Size of Abrasive, Stand-Off-Distance, and Temperature of Abrasive on Deformation and Stress Generated on the Work piece Due to the Impact of Jet. Simulation result for maximum stress profile at the target impact zone of jet and the deformation due to the stress generation has been displayed below in Figure 5- 6.

Table 4: Taguchi simulation matrix for Stress and deformation at target zone

Run No	Angle	Velocity	SOD	Grain Size	Stress (MPa)	Deformation (mm)
1	65	250	4	245	0.8765	1.7345
2	65	280	6	445	0.7745	1.5674
3	65	310	8	645	0.7323	1.3456
4	65	340	10	845	0.7156	1.2280

5	75	250	6	645	0.9123	2.6543
6	75	280	4	845	0.9056	2.7654
7	75	310	10	245	0.8996	2.6243
8	75	340	8	445	0.8134	2.6432
9	90	250	8	845	1.1127	4.0947
10	90	280	10	645	0.9481	3.5315
11	90	310	4	445	1.2839	4.8157
12	90	340	6	245	1.1983	4.1736
13	105	250	10	445	1.0087	3.4543
14	105	280	8	245	0.9765	3.9191
15	105	310	6	845	0.9123	3.9765
16	105	340	4	645	0.8995	3.9982

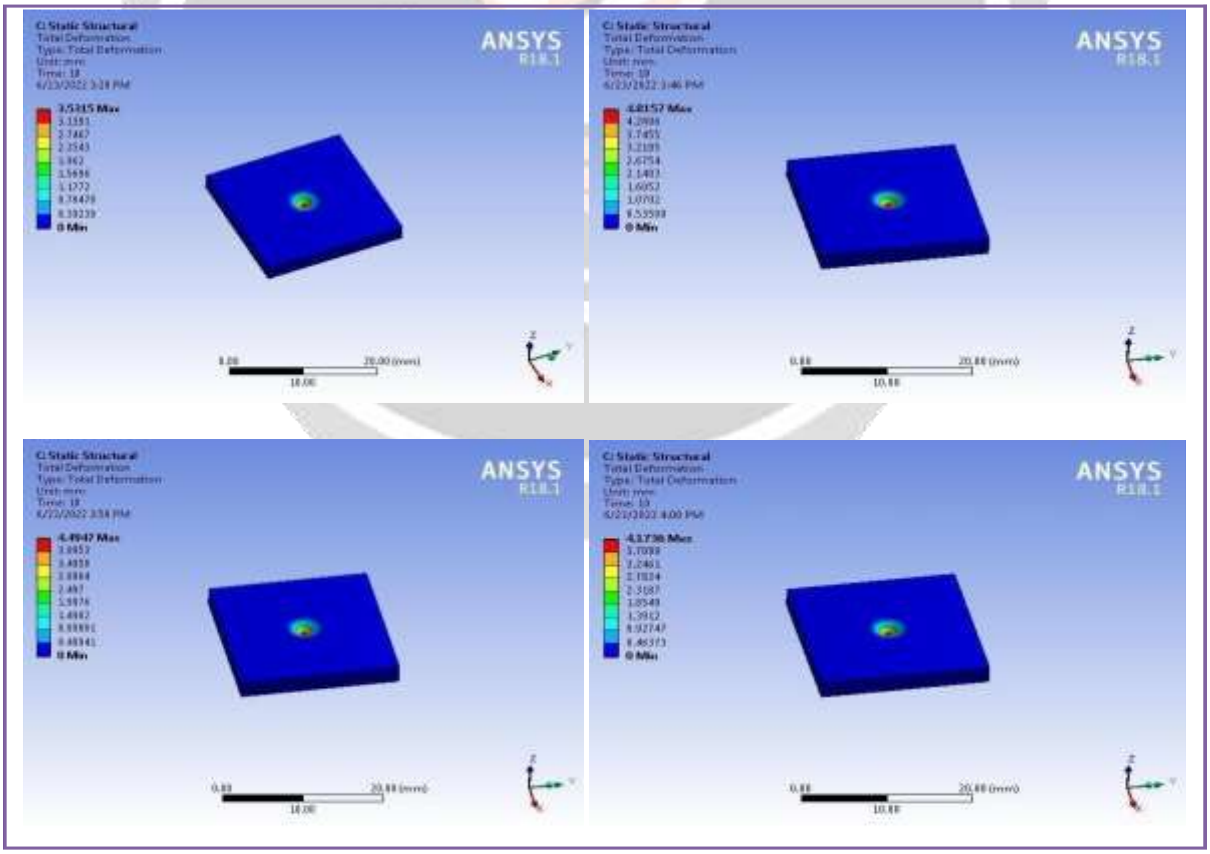

Fig.5 Deformation Contour Profile different Parameter

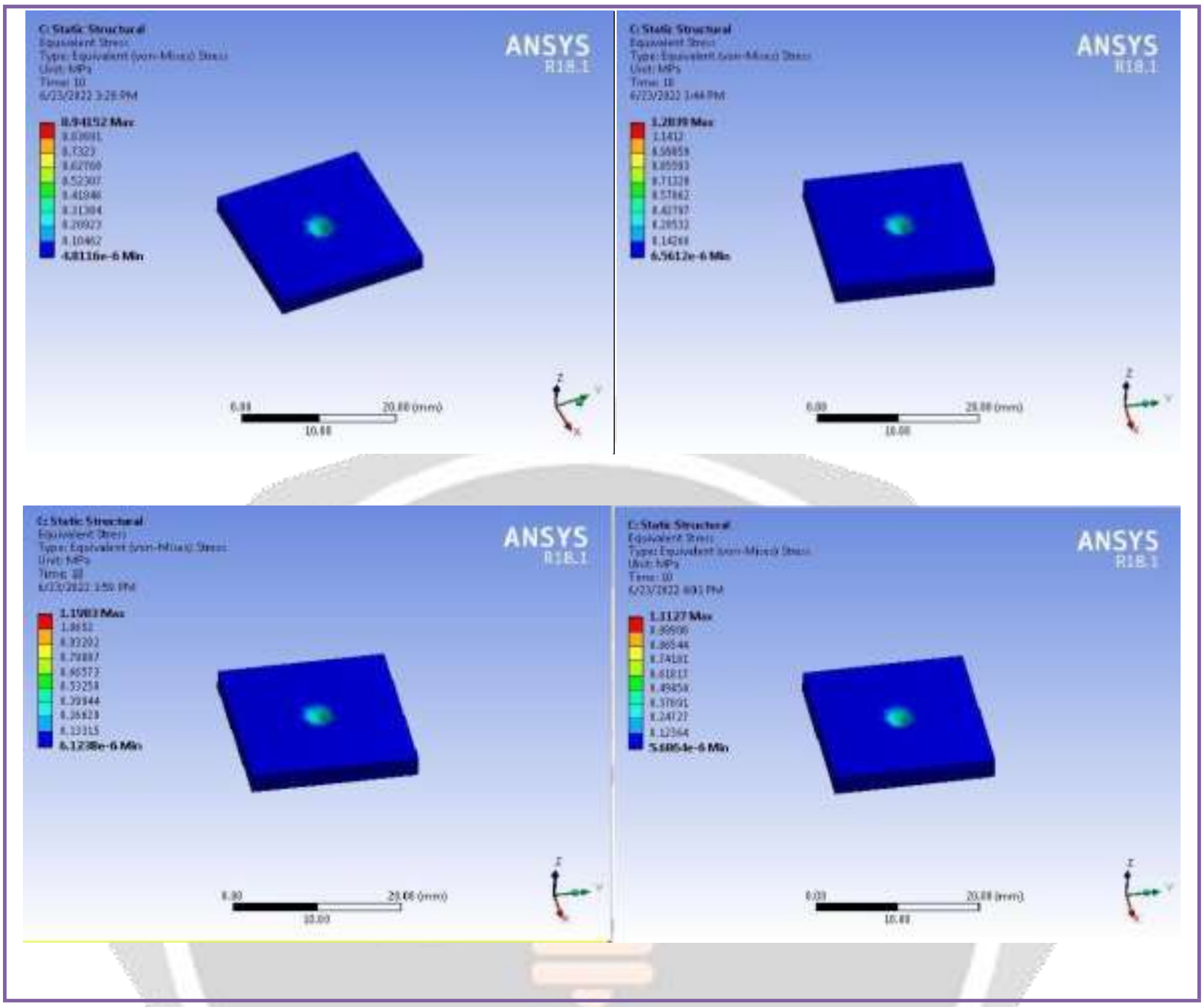

Fig.6 Stress Profile contour at different Parameter

4.3 Effect of Velocity of Jet, Grain Size of Abrasive, Stand-Off-Distance, and Impact angle of abrasive jet on Erosion Rate at the Target Surface of the Work piece: Simulation result for erosion profile at the target impact zone of jet on the work piece has been displayed below in Figure 7-12.

Table 5: Taguchi simulation matrix for simulated erosion rate at target zone.

Run No	Angle	Velocity	SOD	Grain Size	Material Erosion (Gram/m^2-sec)
1	65	250	4	245	0.000564
2	65	280	6	445	0.000431
3	65	310	8	645	0.000229
4	65	340	10	845	0.000193
5	75	250	6	645	0.000765

6	75	280	4	845	0.000851
7	75	310	10	245	0.000721
8	75	340	8	445	0.000815
9	90	250	8	845	0.00291
10	90	280	10	645	0.00186
11	90	310	4	445	0.00386
12	90	340	6	245	0.00354
13	105	250	10	445	0.00107
14	105	280	8	245	0.00165
15	105	310	6	845	0.00267
16	105	340	4	645	0.00298

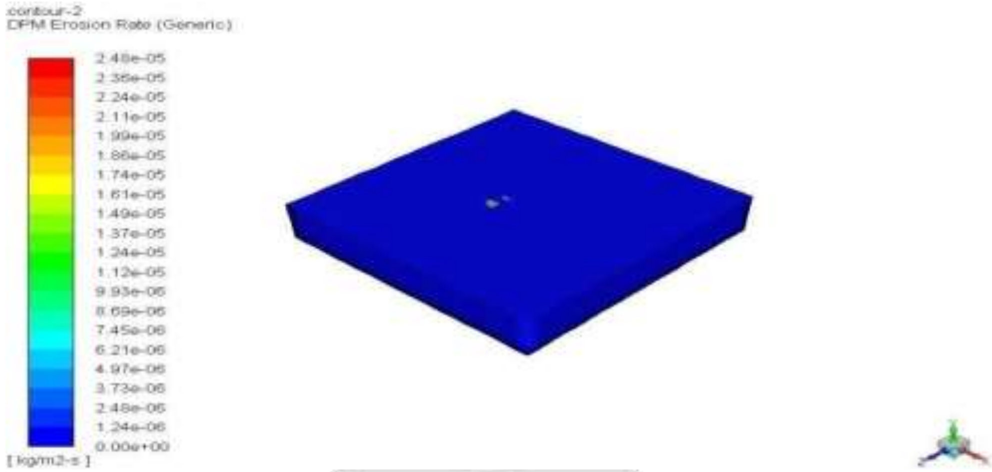
contour-2
DPM Erosion Rate (Generic)
2.48e-05
2.36e-05
2.24e-05
2.11e-05
1.99e-05
1.86e-05
1.74e-05
1.61e-05
1.49e-05
1.37e-05
1.24e-05
1.12e-05
9.93e-06
8.69e-06
7.45e-06
6.21e-06
4.97e-06
3.73e-06
2.48e-06
1.24e-06
0.00e+00
[kg/m2-s]

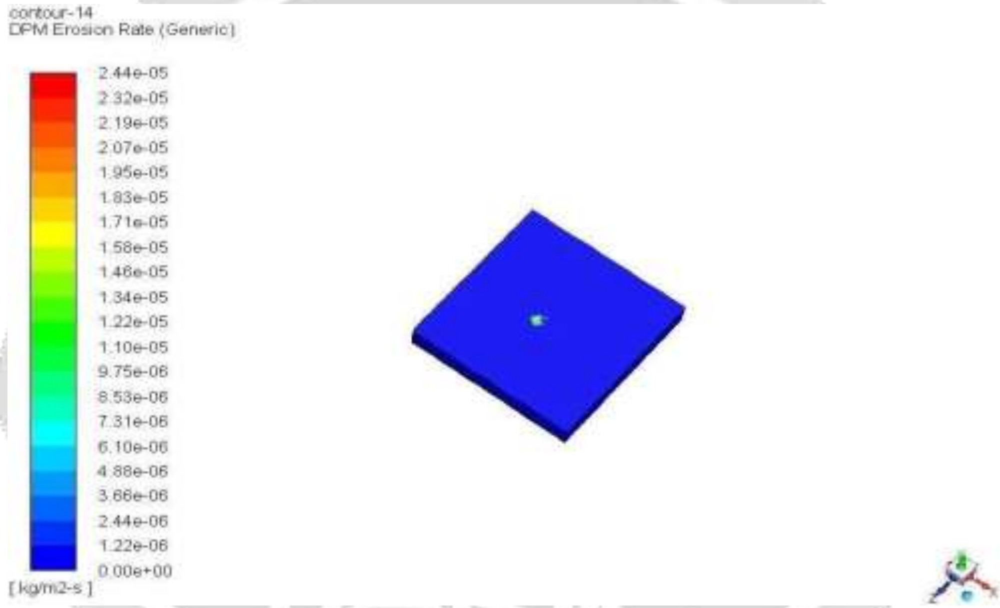
contour-14
DPM Erosion Rate (Generic)
2.44e-05
2.32e-05
2.19e-05
2.07e-05
1.95e-05
1.83e-05
1.71e-05
1.58e-05
1.46e-05
1.34e-05
1.22e-05
1.10e-05
9.75e-06
8.53e-06
7.31e-06
6.10e-06
4.88e-06
3.66e-06
2.44e-06
1.22e-06
0.00e+00
[kg/m2-s]


contour-5
DPM Erosion Rate (Generic)
2.12e-05
2.01e-05
1.90e-05
1.80e-05
1.69e-05
1.59e-05
1.48e-05
1.38e-05
1.27e-05
1.16e-05
1.06e-05
9.52e-06
8.46e-06
7.40e-06
6.35e-06
5.29e-06
4.23e-06
3.17e-06
2.12e-06
1.06e-06
0.00e+00
[kg/m2-s]

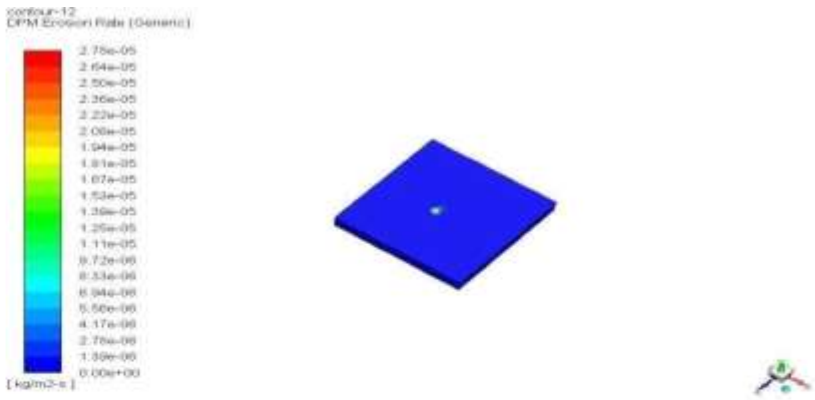

Fig.7-12 Material Erosion Profile at different Parameter

---

5. CONCLUSION

The pressure at the impact zone of heated abrasive jet, erosion at the target impact zone of jet, erosion inside the nozzle surface and deformation due to stress resulting from the simulation of AWJM of K-60 ceramic using SiC abrasive was performed. The results of simulation approach display minor variations if we compare the responses, which are getting from simulation using SiC. The following points are determined in this research.

- Induced pressure at the impact zone of jet is directly proportional to velocity of jet, maximum grain size of abrasive, perpendicular jet impingement angle, i.e. By increasing the velocity of jet, and abrasive grain size maximum pressure is generated on the target zone but for getting maximum pressure at that surface stand-off distance should be small.
- Target material erosion per hot abrasive particle was shown proportional to the abrasive kinetic energy of the particles with minimum stand-off distance in order to avoid the deep chipping formation on the target zone.
- In order to reduce the erosion inside the nozzle surface optimum velocity of jet with moderate grain size o of abrasive should be maintained for compensating the erosion rate at the target zone on the work piece.
- As we know that erosion takes places due to deformation of material, which is generated by stress. So stress is directly proportional to the velocity of jet, perpendicular (900) with maximum grain size of abrasive by maintaining smaller stand-off-distance.

---

6. REFERENCES

1. Messa, G., & Malavasi, S. (2018) “A CFD based method for slurry erosion prediction”, Wear 39899: 127145.

2. Shafiei, N., Getu, H., Sadeghian, A., & Papini, M. (2009) “Computer simulation of developing abrasive jet machined profiles including particle interference”, Journal of Materials Processing Technology 209: (43664378).

3. Jha, S., & Jain, V, K. (2006) “Modeling and Simulation of surface roughness in magneto rheological abrasive flow finishing (MRAFF) process”, Wear 261: 856-866.

4. Jain, R, K., & Jain, V, K. (1999) "Simulation of surface generated in abrasive flow machining", Robotics and computer integrated manufacturing 15: 403-412.

5. Fang, Li., Zhao, J., Sun, K., Zheng, D & Ma, D.(2009) "Temperature as sensitive monitor for efficiency of work in abrasive flow machining", Wear 266: 678-687.

6. Qi, H., Wen, D., Yuan, Q., Zhang, Li., & Chen, Z. (2017) "numerical investigation on particle impact erosion in ultrasonic-assisted abrasive slurry jet micro machining of glass" Powder Technology 314: 627-634.

7. Chopade, C, S. (2017) "A review on nozzle wears using CFD analysis in abrasive water jet machining", Vishwakarma journal of engineering research: volume1 issue3.

8. Frank, T. (2005) "Advances in Computational Fluid Dynamics (CFD) of 3-dimensional Gas-Liquid Multiphase Flows", NAFEMS Seminar: Simulation of Complex Flows (CFD).

9. Liu, H., Wang, J., Kelson, N., & Brown, R, J. (2004) "A study of abrasive water jet characteristics by CFD simulation", Journal of Materials Processing Technology 153– 154: 488–493.

10. Nouhi, A., Kowsari, K., Spelt, J, K., & Papini, M. (2017) "Abrasive jet machining of channels on highlycurved glass and PMMA surfaces", wear 356-357:30–39.

11. Jain, S., Rathi, R., & Sunar, B. (2017) "Numerical simulation for hydrodynamic characteristics of nozzle used in water jet machining" Publication at: https://www.researchgate.net/publication/316619031

12. Venugopal, S., Chandrasekhar, M., Muthuraman, V., & Satish, S. (2017) "Computational Fluid Dynamics Analysis of Nozzle in Abrasive Water Jet machining", IOP Conf. Series: Materials Science and Engineering 183: 012021 doi:10.1088/1757- 899X/183/1/012021.

13. Prisco, U., & D' Onofrio, M, C. (2008) "Three dimensional CFD simulation of two- phase flow inside the abrasive water jet cutting head", International journal for computational methods in engineering science and mechanics, 9:5, 300-309.

14. Jesthi, D. K., Nayak, R. K., Nanda, B. K., & Das, D. (2019). "Assessment of abrasive Jet Machining of Carbon and Glass Fiber Reinforced Polymer Hybrid Composites." Materials Today: Proceedings 18, 3116–3121.

15. Monoranu, M., Ashworth, S., M'Saoubi, R., Fairclough, J. P., Kerrigan, K., Scaife, R. J., Barnes, S., & Ghadbeigi, H. (2019). "A Comparative Study of the Effects of Milling and Abrasive Water Jet Cutting on Flexural Performance of CFRP." Procedia CIRP 85,277–283.

16. Jagannath N., Hiremath S., & Sadashivappa K. (2012). "Analysis and Parametric Optimizationof Abrasive Hot Air Jet Machining For Glass Using Taguchi Method and Utility Concept", International journal of Mechanical and Material Engineering (IJMME),Vol.7 No. 1, 9-15.

17. Jagannatha N., Hiremath S., Sadashivappa K., & Arun K. V. (2012). "Machining of Soda Lime Glass Using Abrasive Hot Air Jet", Machining Science and Technology, 16:,459-472.

18. Pahuja, R., & Ramulu, M. (2019). "Study of Surface Topography in Abrasive Water Jet Machining of Carbon Foam and Morphological Characterization Using Discrete Wavelet Transform." Journal of Materials Processing Technology 273(January), 116249.

19. Srivastava, A. K., Nag, A., Dixit A. R., Scucka, J., Hloch, S., Klichová, D., Hlaváček, P., & Tiwari, S. (2019). "Hardness Measurement of Surfaces on Hybrid Metal Matrix Composite Created by Turning Using an Abrasive Water Jet and WED." Measurement: Journal of the International Measurement Confederation 131, 628–639.

20. Nanda, B. K., Das, D., Nayak R. K., Mishra, S. B., Routara, B. C., & Dhupal D. (2019). "Fluidised Bed Hot Abrasive Jet Machining of Borosilicate Glass with Zircon Sand." Materials Today: Proceedings 18, 2993– 3000.

21. Thakur, R. K., Singh, K. K., & Ramkumar, J. (2020). "Experimental Investigation of Abrasive Waterjet Hole Cutting on Hybrid Carbon/Glass Composite." Materials Today: Proceedings 21,1551-1558.

22. Reddy, V. N., & Venkatesh, B. (2019). "Optimization of Parameters in Abrasive Water Jet Machining of Glass Laminate Aluminium Reinforced Epoxy (GLARE)." Materials Today: Proceedings 19,890–894.

23. Ghazavi, A., & Papini, M. (2019). "An Inverse Method for the Abrasive Jet Micro- Machining of High Aspect Ratio Channels of Desired Topography – Part II, Experiments." Precision Engineering 58(April), 25–34.

24. Verma, K., V, Anandakrishnan, & Sathish, S. (2020). "Modelling and Analysis of Abrasive Water Jet Machining of AA2014 Alloy with Al2O3 Abrasive Using Fuzzy Logic." Materials Today: Proceedings 21, 652–657.

25. Jeykrishnan, J., Ramnath, B. V., Vignesh, S. S., Sridharan, P., & Saravanan, B. (2019)."Optimization of Process Parameters in Abrasive Water Jet Machining/Cutting (AWJM) of Nickel Alloy Using Traditional Analysis to Minimize Kerf Taper Angle." Materials Today: Proceedings 16, 392–397.

26. Uhlmann, E., Schmiedel, C., & Wendler, J. (2015) "CFD simulation of abrasive flow machining process", Procedia CIRP 31: 209 – 214.

27. . Fan. J., Fan, C., & Wang, J. (2011) "Flow Dynamic Simulation of Micro Abrasive Water Jet", Solid state phenomena Vol 175, pp: 171-176.

28. Verma, S., Mishra, S, K., & Mallick, S, K. (2012) "CFD analysis of nozzle in abrasive water suspension jet machining", International Journal of Advanced Engineering Research and Studies: https://www.researchgate.net/publication/327954624 .

29. . Deepak, D., Anjaiah, D., Karanth, K, V., & Sharma, N, Y. (2012) "CFD Simulation of Flow in an Abrasive Water Suspension Jet: The Effect of Inlet Operating Pressure and Volume Fraction on Skin Friction and Exit Kinetic Energy", Hindawi Publishing Corporation: Advances in Mechanical Engineering Volume 2012, Article ID 186430, 8 pages doi:10.1155/2012/186430.

30. . Liu, H., Wang, J., Brown, R, J., & Kelson, N. (2003) "Computational Fluid Dynamic (CFD) Simulation of Ultrahigh Velocity Abrasive Water jet", Key Engineering Materials, Vols. 233-236, 477-482.